Indones. J. Chem., 2022, 22 (5), 1205 - 1217

1205

Role of Temperature and Exposure Time for Controlled and Accelerated Synthesis of Graphene Oxide Using Tour Method

Uswatul Chasanah[1], Wega Trisunaryanti[1*], Haryo Satriya Oktaviano[2],
Triyono Triyono[1], and Dyah Ayu Fatmawati[1]

[1]*Department of Chemistry, Faculty of Mathematics and Natural Sciences, Universitas Gadjah Mada,*
Sekip Utara, Yogyakarta 55281, Indonesia

[2]*Research & Technology Center, PT. Pertamina (Persero), Sopo Del Tower A, Floor 51,*
Jl. Mega Kuningan Barat III, Kawasan Mega Kuningan, Jakarta Selatan, DKI Jakarta, 12950, Indonesia

Abstract: *Synthesis of graphene oxide (GO) with the Tour method has been studied. In this procedure, phosphoric acid was mixed with sulfuric acid in the ratio of 1:9, and then potassium permanganate and graphite with the ratio of 6:1 was added in an ice bath at the variation of oxidation times of 1, 7 and 24 h and temperatures of 40, 50 and 60 °C. The GOs were characterized by UV–Visible spectroscopy, Fourier Transform InfraRed (FT-IR) spectroscopy, X-ray Diffraction (XRD), Scanning Electron Microscopy-Energy Dispersive X-Ray (SEM-EDX), and Transmission Electron Microscopy (TEM). The results show that the GO oxidized at 40 °C for 7 h (GO-7-40) has been successfully formed indicating that GO-7-40 is the most efficient GO. The GO-7-40 is characterized by a peak at $2\theta = 10.89°$ in the XRD diffractogram, resulting calculation of the average distance between graphene layer (d) of 0.81 nm. The average number of graphene layers (n) is 4, the oxidation level (C/O) is 1.50 according to EDX data, λ_{max} at 226 nm attributes to $\pi \rightarrow \pi^*$ transitions of C=C bond in UV-Vis spectrum, and the functional groups such as O-H, C=C, C-OH, and C-OC are observed in FT-IR spectrum.*

Keywords: *graphene oxide; oxidation time; temperature; Tour method*

■ INTRODUCTION

Graphene oxide (GO) is a single-layer graphene nanosheet bonded with functional groups containing oxygen and is part of carbon material derivatives [1]. Graphene oxide displays some outstanding properties, such as high thermal conductivity, specific surface area and electrical conductivity [2]. The high electrical conductivity of graphene is due to zero-overlap semimetal with electrons and holes as charge carriers. Each carbon atom has six electrons, and the four outermost electrons are available for chemical bonding, but in the 2-D plane, each atom is connected to three other carbon atoms, and one electron is freely available for electronic conduction in the 3-D space [3]. It has received much attention for use as an adsorption material and in catalytic applications, owing to its suitable adsorbents and photonic properties

for catalysis, which can improve the photocatalytic properties of materials [4]. Graphene oxide is usually also used as antibiotics [5], chemical sensors [6], and in the removal of organic dyes [7] as well as heavy metal ions [8].

Graphene oxide can be synthesized by the chemical vapor deposition (CVD) as one of the effective techniques for the preparation of low-defect density and enhanced large area monolayer or film-layer graphene films. However, the CVD technique consumes time, uses large amounts of high purity gases and demands high energy input. Plasma enhanced CVD utilizes lower processing temperature. However, producing high-quality graphene with enhanced surface area with fewer defects remains challenging [9]. The other choice, GO can be produced from the oxidation and exfoliation of

graphite, generally in an aqueous solution, yielding hydrophilic carbon-based sheets that are decorated with various oxygenated functional groups [10]. Synthesis of graphene with high quality from graphite can be done with the chemical exfoliation method [11]. This technique combines the oxidation of graphite followed by the reduction process to produce graphene nanosheets. The oxidation of graphite is spread over a long period. Benjamin Collins Brodie [12] has reported that the addition of potassium chlorate ($KClO_3$) to the graphitic compound in nitric acid (HNO_3) provides an increase in the weight of the sample due to the incorporation of hydrogen (H) and oxygen (O). Another method of graphite oxidation has been reported by Staudenmaier [13] with still emphasizing the use of sulfuric acid (H_2SO_4) and a high amount of potassium chlorate ($KClO_4$). Meanwhile, Hummers and Offeman [14] have proposed the use of potassium permanganate ($KMnO_4$) and sulfuric acid as reagents. The H_2SO_4 acts as an intercalation agent stabilizing the oxidant and solvent to transport the oxidant into the graphite interlayers [15]. This approach differs from Brodie method [12], particularly regarding to the reagents and the time of the reaction. Also, the Hummers method requires a step to remove the excess permanganate ions and stop the oxidation reaction using hydrogen peroxide [16]. In the Hummers method, $KMnO_4$ is used to replace $KClO_3$ to avoid spontaneous explosion during the oxidation process, while $NaNO_3$ replaced fuming HNO_3 to eliminate fog acid produced. This process takes just in few hours to produce high-quality GO. The Hummers method still has flaws, whereby it produces toxic gas such as NO_2 and N_2O_4 because of the use of $NaNO_3$ [17].

Marcano et al. [10] have completed the study on the differences among the Hummers method, modified Hummers method, and improved Hummers method without $NaNO_3$. In 2010, Tour et al. [18] reported an improvement in the Hummers method by excluding $NaNO_3$ to prevent the generation of toxic gases, using ice instead of liquid water to prevent the high-temperature rise, thus promoting better and easier control of the process, and also increasing the yield and degree of oxidation, together with promoting the retention of

carbon rings in the basal plane by introducing phosphoric acid (H_3PO_4) to the reaction media. The Tour method is based on the dispersing of graphite in a mixture of concentrated sulfuric and phosphoric acids in a volume ratio of 9:1 and further oxidation of graphite by potassium permanganate [19]. The Tour method eliminates the production of toxic gases and produces a more oxidized graphite oxide with a more regular carbon framework and larger sheet size [20]. Another advantage of the Tour method is to produce a higher yield of heavily oxidized hydrophilic GO [21-22].

According to researchers [23-25], various modifications of the Tour methods can be carried out using different amounts of graphite, oxidant concentrations, oxidation time, and temperature used. Temperature affects the formation of single-layer GO [26]. Many reports that provide a detailed procedure for the synthesis of GO were analyzed based on this perspective. For example, Olorunkosebi et al. [27] allowed this step to prolong with various oxidation times 11, 12, 13, and 14 h at 50 °C. Sali et al. [16] studied temperature of 30 °C but used oxidation time of 72 h. Habte and Ayele [28] maintained the temperature of the system at 50 °C for 12 h, while Benzait et al. [24] synthesized GO at temperature below 10 °C for 24 h. Ranjan et al. [29] concluded that good quality GO samples can be synthesized through Tour method at 65 °C with the oxidation time of 24 h This strategy did not have any Mn and spurious carbonaceous residues without the need for any sophisticated filtration protocol. Meanwhile, Kang et al. [30] adopted the Hummers method and investigated it with three time-variables (2, 4 and 8 h) and three temperature-variables (45, 70 and 95 °C) resulting in GO at 45 °C for 8 h.

There have been many studies on GO synthesis with various oxidation times and/or temperatures. The oxidation time used is quite long (above 8 h) and the temperature used is quite high. Therefore, this study suggests a new insight for studying temperature and oxidation time using the Tour method. Reducing oxidation time and temperature can improve the green chemistry aspect. This research is expected to get an effective and efficient method for producing more GO.

■ **EXPERIMENTAL SECTION**

Materials

Hydrochloric acid (37% HCl), sulfuric acid (98% H_2SO_4), graphite, phosphoric acid (85% H_3PO_4), potassium permanganate ($KMnO_4$), hydrogen peroxide (30% H_2O_2), silver nitrate ($AgNO_3$), barium chloride ($BaCl_2$), and ethanol were purchased from Merck. The deionized water was obtained from One-med, while bi-distilled water and phosphate-buffered saline (PBS) was utilized for the washing process.

Instrumentation

X-ray diffraction (XRD) measurement was performed on a Bruker D2 Phaser diffractometer using the Cu Kα as the irradiation (k = 0.15405 nm) at a 2θ scan range of 5–90° to detect the crystal size. The functional group of GO was characterized by Fourier transform infrared (FTIR) spectrophotometer (Shimadzu Prestige 21, FTIR impact 410) with a range of 400–4000 cm^{-1} using KBr pellets. The surface morphology of GO was examined by Scanning Electron Microscope (SEM, JEOL JSM-6510). Graphene nanosheet structure was determined by transmission electron microscopy (TEM, JEOL JEM-1400). The electronic transition condition of GO was measured by UV-Vis Spectrophotometer 1800 from Shimadzu Scientific.

Procedure

Our method was adapted from Benzait et al. [24] and Ranjan et al. [29] methods with certain crucial modifications (Fig. 1). Initially, graphite powder and $KMnO_4$ (1:6 %w/w) were mixed in a mortar and pestle for 5 min and kept at a temperature below 5 °C. A separate solution of H_2SO_4 and H_3PO_4 (9:1 %v/v) was prepared and also kept at a temperature below 5 °C. The acid solution was then added to the mixture of graphite powder and $KMnO_4$ with continuous stirring (using a magnetic stirrer). The solution obtained was heated at 65 °C and was left with variation times of 1, 7 and 24 h with continuous stirring denoted as GO-1-65, GO-7-65, and GO-24-65. After the stirring process, the solution was
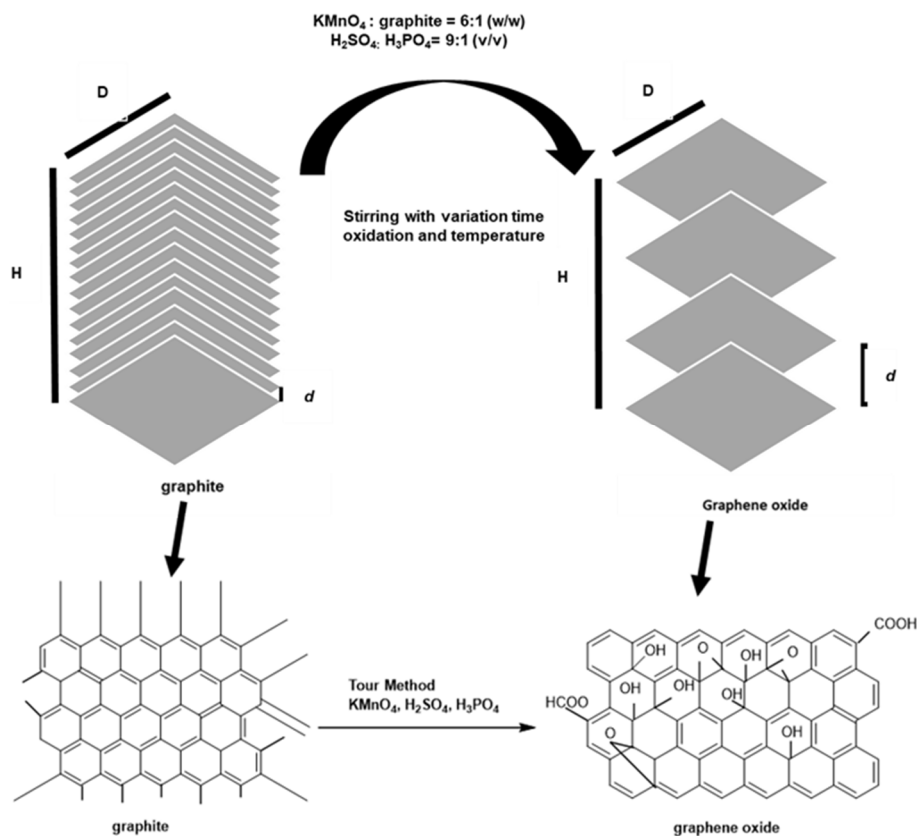

Fig 1. The illustration of Tour method

allowed to cool to room temperature. This was then added to a beaker containing 200 mL of deionized water and ice. Then, 4 mL of H_2O_2 was added while stirring the mixture with a glass rod. The purpose of H_2O_2 was to stop the oxidation reaction and to reduce the residual $KMnO_4$ to soluble manganese sulfate ($MnSO_4$) in an acidic medium, as described in Eq. (1) [28]:

$$2KMnO_4 + 5H_2O_2 + 3H_2SO_4 \rightarrow 2MnSO_4 + K_2SO_4 \\ + 8H_2O_{(steam)} + 5O_2 \tag{1}$$
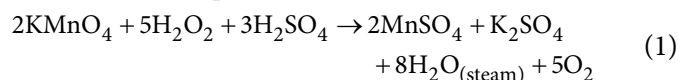
When H_2O_2 was added, bubbling occurred, and a bright yellow color was observed, indicating a high level of oxidation. The mixture was washed with HCl (2 times) and ethanol (2 times) with intermediate centrifugation (at 5,000 rpm for 5 min). The precipitate was washed with PBS until pH 7. The neutral solution was checked by $AgNO_3$ to detect the presence of SO_4^{2-} ion and $BaCl_2$ to detect the presence of Cl^- ion. The solution was rewashed using bi-distilled water until the solution was free of both ions. The precipitate formed was dried at 70 °C for 24 h. The step was repeated with variation temperatures at 40, 50 and 60 °C for 7 h, denoted as GO-7-40, GO-7-50, and GO-7-60.

■ RESULTS AND DISCUSSION

Diffractograms of graphite and all GO samples are shown in Fig. 2. The XRD pattern of graphite shows a peak at 2θ = 26.21° (hkl 002) according to the pattern of JCPDS standard graphite diffraction No.75-2078. Graphite has a sharp peak with high intensity, which

indicates that graphite has good crystallinity. It is in line with the structure of graphite, which is composed of carbon atoms bonded together and fully conjugated sp^2 to form honeycomb-like crystals [31]. However, after the graphite is oxidized, the crystal undergoes a structural change or defect due to oxygen functional groups from the permanganate oxidizing agent. As the consequence, there is a change in the conjugation of some carbons from sp^2 to sp^3, causing the crystallinity to decrease and the peak to be broader (amorphic of the material appears). The broadening effect of the peak is probably due to the formation of complex epoxidation of oxygenated unsaturated groups throughout the graphene layer, which distorts the lattice in the stacking order of the graphite [32]. The infiltration of oxygen functional groups between the graphene sheets in the graphite structure also resulted in an increase in the distance between the sheets from 0.34 to ~0.9 nm. Therefore, the 2θ angle seen in the XRD spectra also shifted from ~26° to ~9°. The peaks are associated with d = 0.8–0.9 nm due to the presence of chemical groups onto the graphene basal plane, so the d of GO depends on the degree of oxidation of graphite and the number of water molecules intercalation between the oxidized graphene layers [33].

Increasing the oxidation time, the XRD pattern of GO-1-65, GO-7-65, and GO-24-65 shows the intensity of the peak at 2θ of 9.78, 9.59, and 9.39°, respectively, but the interlayer spacing (d) does not significantly change
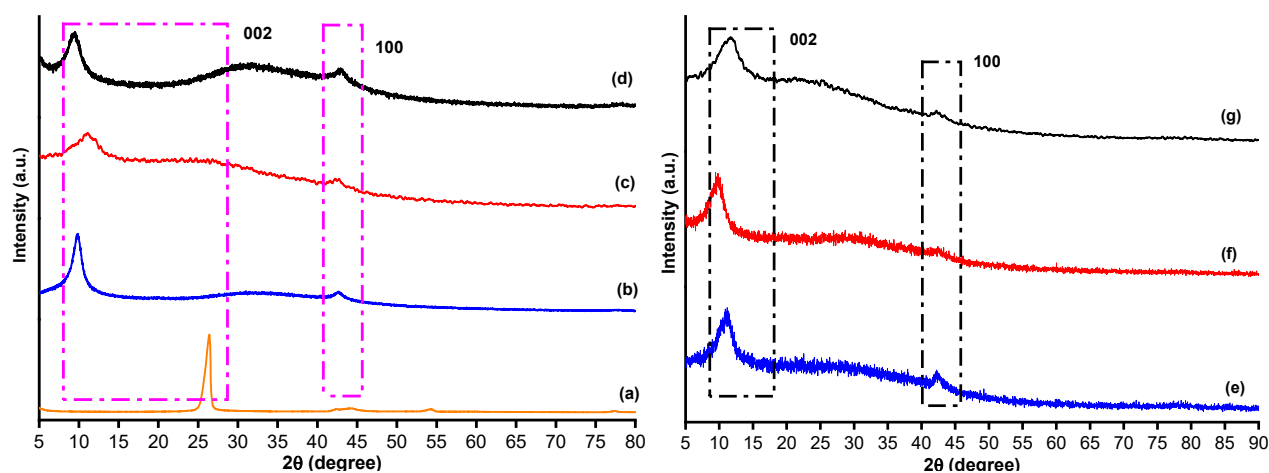

Fig 2. Diffractogram of (a) graphite, (b) GO-1-65, (c) GO-7-65, (d) GO-24-65, (e) GO-7-40, (f) GO-7-50, (g) GO-7-60

about 0.9 nm. Meanwhile, GO-7-40, GO-7-50, and GO-7-60 show peaks centered at 10.89, 9.64, and 11.39°, respectively, with d of 0.8–0.9 nm. The results show that the role of temperature can have more effect on the peak in the diffractogram than the oxidation time. Those are consistent with the range values of 9–12° reported in the literature [34-38]. The oxidation time of 7 h was chosen to evaluate the effect of temperature based on the results of UV-Vis analysis which will be described in the following explanation (Fig. 3).

The distance between graphene layers or interlayer spacing (d) from peak (002) reflection was calculated using Bragg equation. Meanwhile, the average height of stacking layers (H) was calculated using Scherrer equation with a constant equal to 0.9. The average diameter of stacking layers (D) was determined by using the Scherrer equation with a Warren constant of 1.84 [39]. The

graphite and GO have a nanostructure dimension size (D×H, see Table 1). The oxidation time of GO-24-65 can just exfoliate graphite until 5–6 layers, although the others GO from oxidation time GO-1-65 (7 layers) and GO-7-65 (6 layers), but from the oxidation temperature of GO-7-60 more can exfoliate graphite until 3 layers whereas GO-7-40 and GO-7-50 can exfoliate graphite just 4 layers, indicating that the oxidation temperature effect has more effect than the oxidation time. The ideal GO has 1 layer. In the other word, the production of GO with a few layers is more expected [40]. Therefore, GO-7-60 has the best graphite exfoliation.

The UV-Vis spectra for graphite and all GO samples in the range of 190–900 nm were investigated in water solution. As we can observe in Fig. 3, the region 400–900 nm is not affected by absorptions. The maximum absorbance for GO-7-65 and GO-24-65 is 243

Table 1. Calculation of H (the average height of samples GO stacking nanolayers), D (average diameter in stacking layers), n (the average number of graphene layers), and d (the average distance between graphene layers) of graphite and GO samples

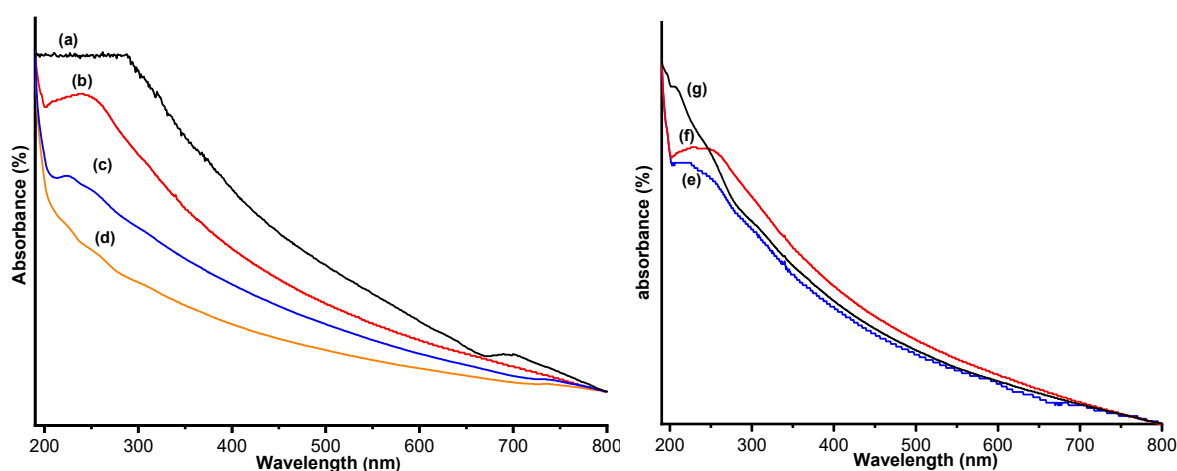| Sample	Peak (002)					Peak (100)		
	2θ (deg)	FWHM (deg)	H (nm)	d (nm)	n	2θ (deg)	FWHM (deg)	D (nm)
graphite	26.21	0.74	11	0.34	32	42.32	0.46	38
GO-1-65	9.78	1.38	6	0.90	7	42.64	1.09	17
GO-7-65	9.59	1.46	6	0.94	6	42.77	1.11	15
GO-24-65	9.39	1.71	4	0.94	5-6	42.95	1.25	14
GO-7-40	10.89	2.39	3	0.81	4	42.34	0.96	18
GO-7-50	9.64	2.04	4	0.92	4	41.47	6.67	13
GO-7-60	11.39	3.27	3	0.78	3	42.127	1.21	14

Fig 3. UV-Vis spectra of (a) graphite, (b) GO-1-65, (c) GO-7-65, (d) GO-24-65, (e) GO-7-40, (f) GO-7-50, (g) GO-7-60

and 226 nm, respectively. However, the peak of GO-1-65 at ~210–240 nm has not emerged yet (Fig. 3(b-d)), probably because the oxidation of 1h does not completely occur or only it was formed graphite oxide. The main difference between graphite oxide and graphene oxide is, thus, the number of layers. While graphite oxide is a multilayer system in graphene oxide (Fig. 4). Hence, the oxidation time of 7 was chosen for the variation of temperature. The maximum absorbance for GO-7-40, GO-7-50, and GO-7-60 (Fig. 3(e-g)) takes place at λ_{max} of 226, 228 and 210 nm, respectively. This band is attributed to π→π* transitions of C=C bond in conjugated systems [41-42]. The lower the absorption peak, the more decreased delocalized electrons are, and it is considered that higher energy is required for the electronic transition. It indicates that the sample is more oxidized with more functional groups on the basal planes [42]. This blue shift in UV-Vis absorption is due to the hybridization of sp^3 carbon atoms and a decrease in the number of electrons [18].

The FTIR analysis (Fig. 5) was carried out to obtain information about the oxygen functionalities incorporated into the graphitic planes due to the oxidation. The IR absorbances are observed in the regions of 1210–1320, 1540–1675 and 1020–1075 cm^{-1} corresponding to the vibrations of C-O from ether and ester, sp^2-hybridized C=C in-plane vibrations, C–O stretching of alcohol (C–OH), and carboxylic acid (C–OC) functional groups, respectively [43–45]. The vibration of the C–OH functional group indicated graphite has successfully oxidized [46]. The spectra still contain C=C vibration because these materials consist of almost sp^2-conjugated carbon, although they have few defects of sp^3-conjugated carbon. All spectra also show a broader IR absorbance in the range 3000–3720 cm^{-1}. The characteristic of O–H stretching modes supports the presence of hydroxyl and carboxyl groups [47]. When the oxidation time of graphite increased from 1 to 24 h, the positions of FTIR bands remains unchanged, indicating that the types of functional groups are independent of the
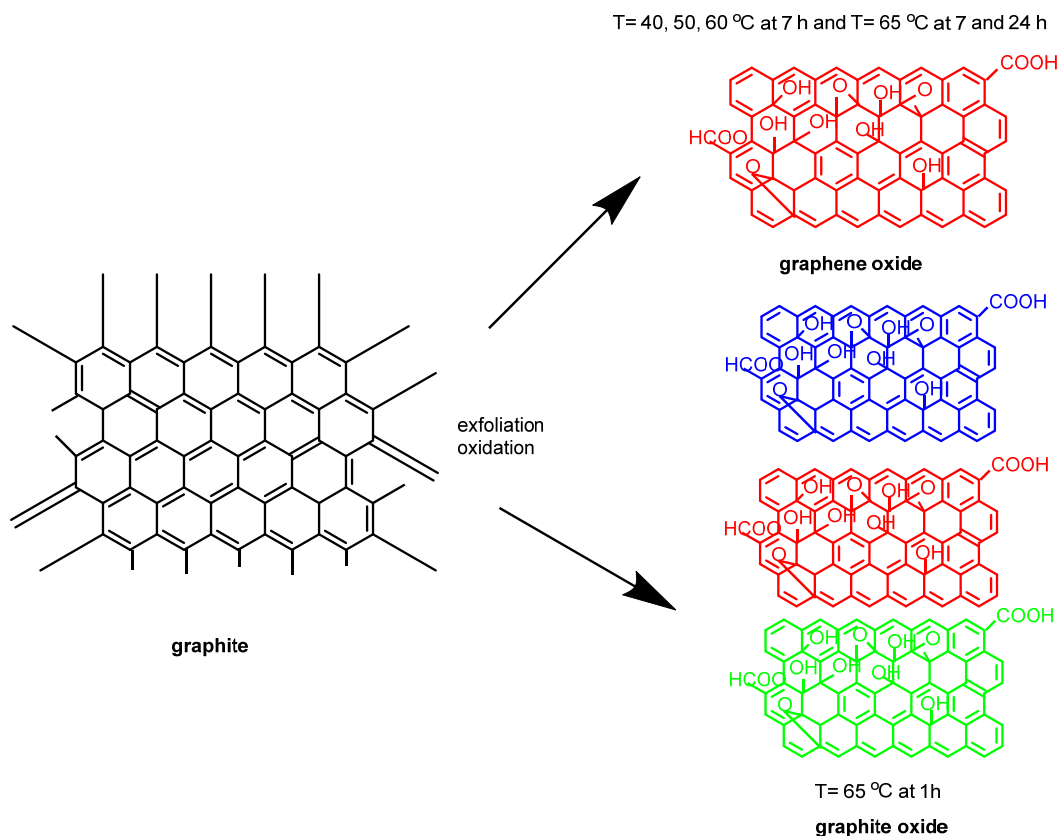

Fig 4. The mechanism of temperature and time oxidation oxide of graphene oxide synthesis

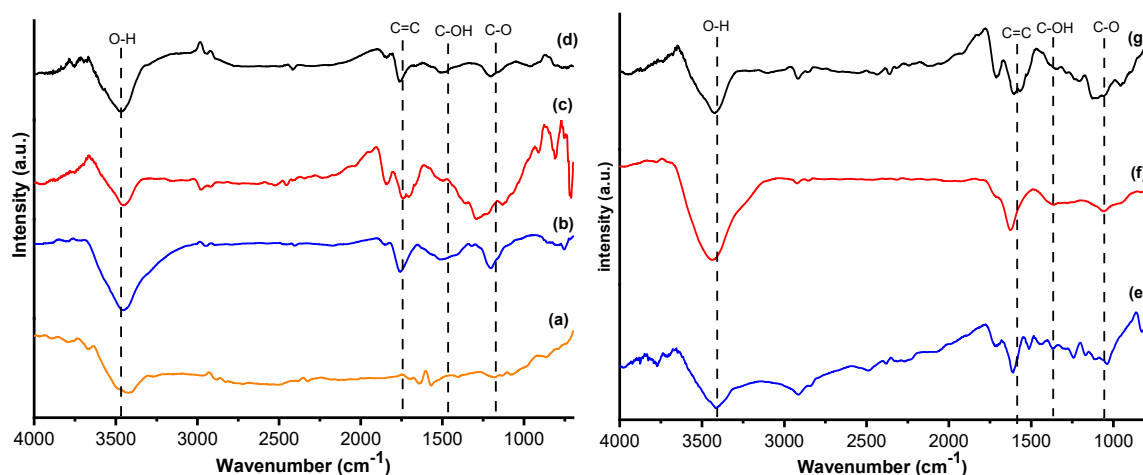*Indones. J. Chem., 2022, 22 (5), 1205 - 1217*

1211

Fig 5. FT-IR spectra of (a) graphite, (b) GO-1-65, (c) GO-7-65, (d) GO-24-65, (e) GO-7-40, (f) GO-7-50, (g) GO-7-60

oxidation time [32]. Similar FTIR pattern is observed for the variation of temperature (40–60 °C). These types of functional groups cause the distance of the graphene layer in graphite structure to increase, confirming the previous XRD data. The presence of various oxygen-containing groups reveals that the graphite has been oxidized. The presence of the polar groups, especially the surface hydroxyl groups, leads to the formation of hydrogen bonds between the graphitic layer and water molecules. This further explains the hydrophilic nature of GO. The detail of absorption peak of O–H, C=C, C-OH, and C–OC functional groups formed analyzed by FTIR can be seen in Table 2.

The morphological aspects of graphite and all GO samples are investigated by using a scanning electron microscope (SEM), as shown in Fig. 6. Here, graphite (Fig. 6(a)) is displayed and exhibits large grains. Unlikely, GO-1-65, GO-7-65, GO-24-65, GO-7-40, GO-7-50, and GO-7-60 morphology consist of tightly packed layers, as

shown in Fig. 6b-g. The distinct morphology is related to the exfoliation process in the first step of synthesis and the re-packing of the material in the solid phase due to the oxygen domains on the graphene basal plane [26]. The micrograph of all GO materials has a porous sponge-like structure with the graphene sheet not well connected. It is an indication that graphite has been exfoliated during the oxidation process. It may be due to the distorted graphene sheets when oxygen and other functional groups are attached to graphene sheets to form GO [48–50]. Fig. 6(b-g) also describe the GOs as thin sheets with a few layered GOs that match the literature [51].

The elemental analysis is evaluated from energy dispersive X-ray (EDX) spectra. The spectrum shows peaks corresponding to C, O, S, Na, K, and Ca. Potassium, sodium, and sulfur were present due to H_2SO_4 and $KMnO_4$ being used as the oxidizing agent, and PBS was used during the washing process. The carbon-oxygen

Table 2. Absorption peaks of graphite and all GO samples

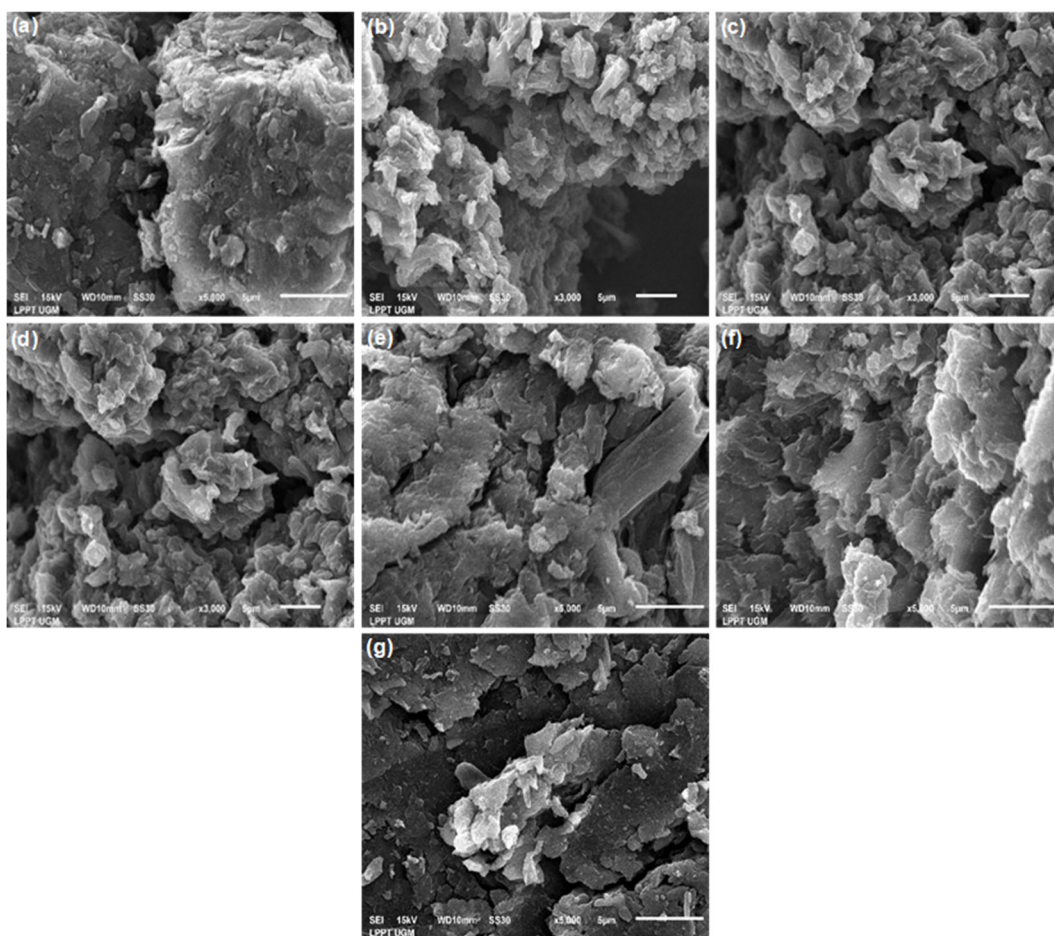| Sample	Functional groups (cm⁻¹)			
	O–H	C=C	C–OH	C–OC
Graphite	3422			
GO-1-65	3421	1624	1369	1035
GO-7-65	3414	1609	1369	1044
GO-24-65	3421	1609	1356	1052
GO-7-40	3436	1603	1376	1031
GO-7-50	3422	1627	1368	1043
GO-7-60	3407	1613	1368	1031

Fig 6. SEM images of (a) graphite, (b) GO-1-65, (c) GO-7-65, (d) GO-24-65, (e) GO-7-40, (f) GO-7-50, (g) GO-7-60

Table 3. The element contained in graphite and GO samples based on EDX

Material	% mass						
	C	O	K	Na	Cl	S	C/O
Graphite	100						∞
GO-1-65	51.72	42.07		4.75	0.17	1.29	1.23
GO-7-65	55.95	39.54		3.08	0.34	1.09	1.41
GO-24-65	52.39	44.86	2.29	3.41	0.32	0.14	1.13
GO-7-40	57.87	38.54	2.72	2.72	0.31	0.57	1.50
GO-7-50	57.32	39.81	0.57	0.34	0.52	1.14	1.44
GO-7-60	57.53	38.87	2.51	0.36		0.73	1.48

ratio (C/O) from GO using the Hummers method is 1.8–2.5 [48-49]. Meanwhile, in the modified Hummers or Tour method, the ratio is 0.7–1.3 [18]. In this work (Table 3), the C/O ratio of GO-7-65 and GO-24-65 are 1.41 and 1.13, respectively, and the C/O ratio of GO-7-40, GO-7-50, and GO-7-60 are 1.50, 1.44, and 1.48, respectively implying high oxidized graphene [50]. The increased

temperature and oxidation time give more oxidized graphene, but there is an outlier datum (GO-1-65). The outlier datum is matched with UV-Vis data which does not appear to peak at 210–240 nm. Instead, from our data, fewer oxidized samples of GO-7-40 and GO-7-60 are found, and this affects the GO properties, e.g., a higher angle at 10.89 and 11.39° in comparison with the

Table 4. Comparison of GO yielding from Hummers method and Tour method

Method	Graphite	Material	Yield	Ref.
Hummers method	3 g	6 $KMnO_4$ H_2SO_4 0.5 $NaNO_3$	3.9 g	[18]
Tour method	3 g	6 $KMnO_4$ 9:1 (H_2SO_4:H_3PO_4)	5.3 g	

average value that is around 9° in XRD diffractogram [26], or the FTIR spectrum.

In contrast with all materials GO, the C/O ratio of graphite is ∞ indicating that graphite does not have impurity since graphite only has carbon element. The results also prove that the exfoliation from graphite to GO is successfully carried out because of the inhibition of the oxygenated groups. The results match with FTIR data.

The TEM micrograph of graphite (Fig. 7(a)) shows major dark areas. All GO samples (Fig. 7(b-g)) show the wrinkled and folded nature of GO sheets [54]. The dark area indicates the thick stacking nanostructure of several graphene layers. The higher transparency area is resulted from stacking nanostructure exfoliation because of the presence of a few amount of oxygen functional groups [55]. Since all GO materials have a light area, so exfoliation of graphite has been successfully conducted.

Table 4 shows that the Tour method has a higher yield GO than the Hummers method. The results match to the literature [21-22] and conclude that the Tour method is more effective and efficient method to produce GO than the Hummers method.

■ **CONCLUSION**

Facile low temperature and reducing the time of GO synthesis have been studied. In XRD data, the oxidation time does not significantly affect the d spacing value compared to oxidation temperature treatment. Both increasing oxidation time and temperature caused the average number of graphene (n) to decrease. The samples of GO-1-65, GO-7-65, GO-24-65, GO-7-40, GO-7-50, and
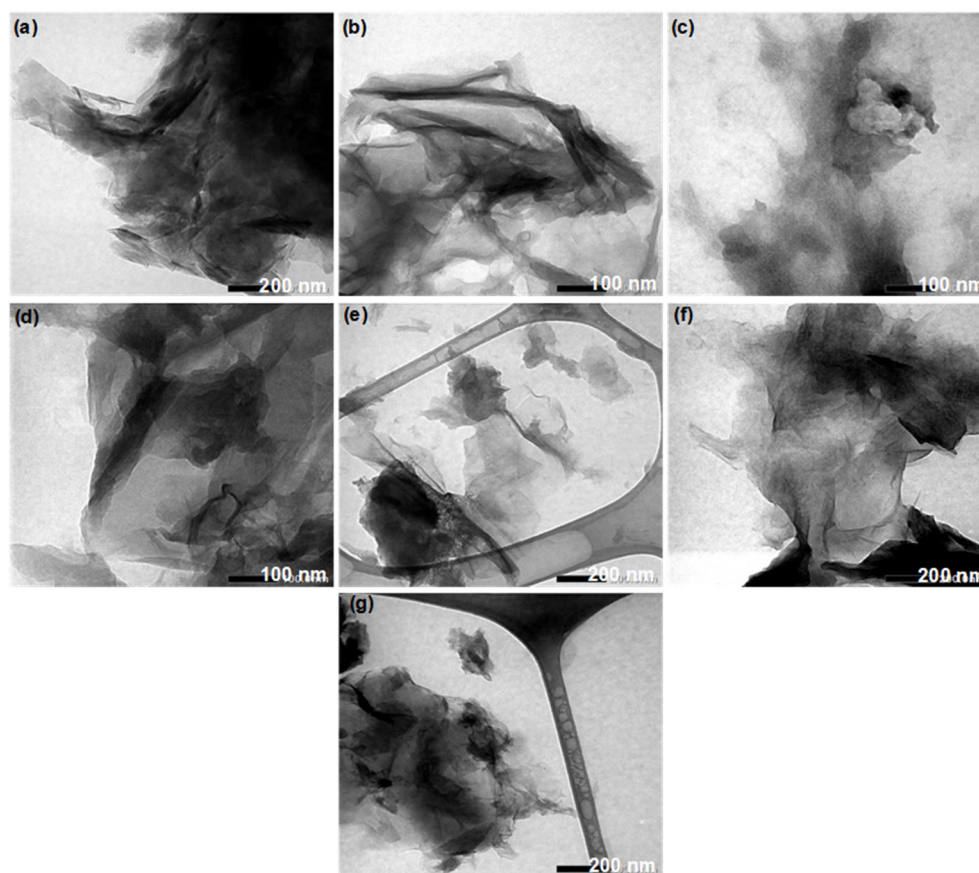

Fig 7. TEM images of (a) graphite, (b) GO-1-65, (c) GO-7-65, (d) GO-24-65, (e) GO-7-40, (f) GO-7-50 (g) GO-7-60

and GO-7-60 show the intensity of the peak at 2θ = 9.78, 9.59, 9.39, 10.89, 9.64, and 11.39°, respectively, with d of 0.8–0.9 nm. The sample of GO-7-60 can exfoliate graphite until 3 layers compared to others such as GO-24-65 which can just exfoliate graphite until 5-6 layers. Then, GO-1-65 (7 layers) and GO-7-65 exfoliate 6 layers, but from the oxidation temperature of GO-7-40 and GO-7-50 can just exfoliate graphite 4 layers. The peaks of UV-Vis spectra indicate all of the samples GO formed except GO-1-65 because the peak does not appear. The peaks of GO-7-65, GO-24-65, GO-7-40, GO-7-50, and GO-7-60 occur at λ_{max} of 243, 226, 226, 228, and 210 nm, respectively. These peaks correspond to $\pi{\rightarrow}\pi^{\star}$ transitions for the C=C aromatic from sp^2 bonding. According to UV-Vis spectra, the higher the oxidation time and temperature, the lower the wavelength formed. The FTIR analysis among all the samples contains the functional groups indicating the formation of GO. The SEM images show GO-1-65, GO-7-65, GO-24-65, GO-7-40, GO-7-50, and GO-7-60 morphology consist of tightly packed layers. The EDX resulted in the increasing oxidation time, and temperature lead the C/O ratio decrease. Based on all of the research results, GO-7-60 shows the best material characteristic among all synthesized GOs because it can exfoliate graphite until 3 layers, close to the ideal graphene, i.e., 1 layer. In addition, synthesis of GO-7-40 has been achieved under lower oxidation temperature, which is in line with the green chemistry principles. From that results, these GO from Tour method can be applied in the removal of organic dye, antibiotics, chemical sensors, and heavy metal ions.

■ ACKNOWLEDGMENTS

■ REFERENCES

[1] Thangavel, S., and Venugopal, G., 2014, Understanding the adsorption property of graphene-oxide with different degrees of oxidation levels, *Powder Technol.*, 257, 141–148.

[2] Georgakilas, V., Otyepka, M., Bourlinos, A.B., Chandra, V., Kim, N., Kemp, K.C., Hobza, P., Zboril, R., and Kim, K.S., 2012, Functionalization of graphene: Covalent and non-covalent approaches, derivatives and applications, *Chem. Rev.*, 112 (11), 6156–6214.

[3] Malik, R., Tomer, V.K., and Chaudhary, V., 2019, "Hybridized graphene for chemical sensing" in *Functionalized Graphene Nanocomposites and Their Derivatives*, Eds. Jawaid, M., Bouhfid, R., and Qaiss, A.K., Elsevier, Amsterdam, Netherlands, 323–338

[4] Gupta, K., and Khatri, O.P., 2017, Reduced graphene oxide as an effective adsorbent for removal of malachite green dye: Plausible adsorption pathways, *J. Colloid Interface Sci.*, 501, 11–21.

[5] Gao, Y., Wu, J., Ren, X., Tan, X., Hayat, T., Alsaedi, A., Cheng, C., and Chen, C., 2017, Impact of graphene oxide on the antibacterial activity of antibiotics against bacteria, *Environ. Sci.: Nano*, 4 (5), 1016–1024.

[6] Saleh, T.A., and Fadillah, G., 2019, Recent trends in the design of chemical sensors based on graphene–metal oxide nanocomposites for the analysis of toxic species and biomolecules, *TrAC, Trends Anal. Chem.*, 120, 115660.

[7] Tan, H.L., Denny, F., Hermawan, M., Wong, R.J., Amal, R., and Ng, Y.H., 2017, Reduced graphene oxide is not a universal promoter for photocatalytic activities of TiO_2, *J. Materiomics*, 3 (1), 51–57.

[8] Gopalakrishnan, A., Krishnan, R., Thangavel, S., Venugopal, G., and Kim, S.J., 2015, Removal of heavy metal ions from pharma-effluents using graphene-oxide nanosorbents and study of their adsorption kinetics, *J. Ind. Eng. Chem.*, 30, 14–19.

[9] Ajala, O.J., Tijani, J.O., Bankole, M.T., and Abdulkareem, A.S., 2022, A critical review on graphene oxide nanostructured material: Properties, synthesis, characterization and application in water and wastewater treatment, *Environ. Nanotechnol. Monit. Manage.*, 18, 100673.

[10] Marcano, D.C., Kosynkin, D.V., Berlin, J.M., Sinitskii, A., Sun, Z., Slesarev, A., Alemany, L.B., Lu, W., and Tour, J.M., 2010, Improved synthesis of graphene oxide, *ACS Nano*, 4 (8), 4806–4814.

[11] Alshamkhani, M.T., Teong, L.K., Putri, L.K., Mohamed, A.R., Lahijani, P., and Mohammadi, M., 2021, Effect of graphite exfoliation routes on the properties of exfoliated graphene and its photocatalytic applications, *J. Environ. Chem. Eng.*, 9 (6), 106506.

[12] Brodie, B.C., 1859, On the atomic weight of graphite, *Philos. Trans. R. Soc. London*, 149, 249–259.

[13] Staudenmaier, L., 1898, Verfahren zur darstellung der draphitsäure, *Ber. Dtsch. Chem. Ges.*, 31, 1481–1487.

[14] Hummers, W.S., and Offeman, R.E., 1958, Preparation of graphitic oxide, *J. Am. Chem. Soc.*, 80 (6), 1339.

[15] Zhu, Y., Kong, G., Pan, Y., Liu, L., Yang, B., Zhang, S., Lai, D., and Che, C., 2022, An improved Hummers method to synthesize graphene oxide using much less concentrated sulfuric acid, *Chin. Chem. Lett.*, 33 (10), 4541–4544.

[16] Sali, S., Mackey, H.R., and Abdala, A.A., 2019, Effect of graphene oxide synthesis method on properties and performance of polysulfone-graphene oxide mixed matrix membranes, *Nanomaterials*, 9 (5), 769.

[17] Zaaba, N.I., Foo, K.L., Hashim, U., Tan, S.J., Liu, W.W., and Voon, C.H., 2017, Synthesis of graphene oxide using modified Hummers method: Solvent influence, *Procedia Eng.*, 184, 469–477.

[18] Marcano, D.C., Kosynkin, D.V., Berlin, J.M., Sinitskii, A., Sun, Z., Slesarev, A.S., Alemany, L.B., Lu, W., and Tour, J.M., 2018, Correction to improved synthesis of graphene oxide, *ACS Nano*, 12 (2), 2078.

[19] Bychko, I., Abakumov, A., Didenko, O., Chen, M., Tang, J., and Strizhak, P., 2022, Differences in the structure and functionalities of graphene oxide and reduced graphene oxide obtained from graphite with various degrees of graphitization, *J. Phys. Chem. Solids*, 164, 110614.

[20] Romero, A., Lavin-Lopez, M.P., Sanchez-Silva, L., Valverde, J.L., and Paton-Carrero, A., 2018, Comparative study of different scalable routes to synthesize graphene oxide and reduced graphene oxide, *Mater. Chem. Phys.*, 203, 284–292.

[21] Chen, J., Li, Y., Huang, L., Li, C., and Shi, G., 2015, High-yield preparation of graphene oxide from small graphite flakes via an improved Hummers method with a simple purification process, *Carbon*, 81, 826–834.

[22] Lavin-Lopez, M.P., Romero, A., Garrido, J., Sanchez-Silva, L., and Valverde, J.L., 2016, Influence of different improved hummers method modifications on the characteristics of graphite oxide in order to make a more easily scalable method, *Ind. Eng. Chem. Res.*, 55 (50), 12836–12847.

[23] Park, J., Cho, Y.S., Sung, S.J., Byeon, M., Yang, S.J., and Park, C.R., 2018, Characteristics tuning of graphene-oxide-based-graphene to various end-uses, *Energy Storage Mater.*, 14, 8–21.

[24] Benzait, Z., Chen, P., and Trabzon, L., 2021, Enhanced synthesis method of graphene oxide, *Nanoscale Adv.*, 3 (1), 223–230.

[25] Boychuk, V.M., Kotsyubynsky, V.O., Bandura, K.V., Yaremiy, I.P., and Fedorchenko, S.V., 2019, Reduced graphene oxide obtained by Hummers and Marcano-Tour methods: Comparison of electrical properties, *J. Nanosci. Nanotechnol.*, 19 (11), 7320–7329.

[26] Pendolino, F., Armata, N., Masullo, T., and Cuttitta, A., 2015, Temperature influence on the synthesis of pristine graphene oxide and graphite oxide, *Mater. Chem. Phys.*, 164, 71–77.

[27] Olorunkosebi, A.A., Eleruja, M.A., Adedeji, A.V., Olofinjana, B., Fasakin, O., Omotoso, E., Oyedotun, K.O., Ajayi, E.O.B., and Manyala, N., 2021, Optimization of graphene oxide through various Hummers' methods and comparative reduction using green approach, *Diamond Relat. Mater.*, 117, 108456.

[28] Habte, A.T., and Ayele, D.W., 2019, Synthesis and characterization of reduced graphene oxide (rGO) started from graphene oxide (GO) using the Tour method with different parameters, *Adv. Mater. Sci. Eng.*, 2019, 5058163.

[29] Ranjan, P., Agrawal, S., Sinha, A., Rao, T.R., Balakrishnan, J., and Thakur, A.D., 2018, A low-cost non-explosive synthesis of graphene oxide for scalable applications, *Sci. Rep.*, 8 (1), 12007.

[30] Kang, J.H., Kim, T., Choi, J., Park, J., Kim, Y.S., Chang, M.S., Jung, H., Park, K.T., Yang, S.J., and Park, C.R., 2016, Hidden second oxidation step of Hummers method, *Chem. Mater.*, 28 (3), 756–764.

[31] Jara, A.D., and Kim, J.Y., 2020, Chemical purification processes of the natural crystalline flake graphite for Li-ion Battery anodes, *Mater. Today Commun.*, 25, 101437.

[32] Suhaimin, N.S., Hanifah, M.F.R., Jusin, J.W., Jaafar, J., Aziz, M., Ismail, A.F., Othman, M.H.D., Abd Rahman, M., Aziz, F., Yusof, N., and Muhamud, M., 2021, Tuning the oxygen functional groups in graphene oxide nanosheets by optimizing the oxidation time, *Phys. E*, 131, 114727.

[33] Meng, L.Y., and Park, S.J., 2012, Preparation and characterization of reduced graphene nanosheets via pre-exfoliation of graphite flakes, *Bull. Korean Chem. Soc.*, 33 (1), 209–214.

[34] Dimiev, A.M., and Tour, J.M., 2014, Mechanism of graphene oxide formation, *ACS Nano*, 8 (3), 3060–3068.

[35] Lee, D.W., De Los Santos V.L., Seo, J.W., Leon Felix, L., Bustamante D.A., Cole, J.M., and Barnes, C.H.W., 2010, The structure of graphite oxide: Investigation of its surface chemical groups, *J. Phys. Chem. B*, 114 (17), 5723–5728.

[36] Dubey, A., Bhavsar, N., Pachchigar, V., Saini, M., Ranjan, M., and Dube, C.L., 2021, Microwave assisted ultrafast synthesis of graphene oxide based magnetic nano composite for environmental remediation, *Ceram. Int.*, 48 (4), 4821–4828.

[37] Roy, O., Jana, A., Pratihar, B., Saha, D.S., and De, S., 2021, Graphene oxide wrapped Mix-valent cobalt phosphate hollow nanotubes as oxygen evolution catalyst with low overpotential, *J. Colloid Interface Sci.*, 610, 592–600.

[38] Shen, B., Lu, D., Zhai, W., and Zheng, W., 2013, Synthesis of graphene by low-temperature exfoliation and reduction of graphite oxide under ambient atmosphere, *J. Mater. Chem. C*, 1 (1), 50–53.

[39] Stobinski, L., Lesiak, B., Malolepszy, A., Mazurkiewicz, M., Mierzwa, B., Zemek, J., Jiricek, P., and Bieloshapka, I., 2014, Graphene oxide and reduced graphene oxide studied by the XRD, TEM and electron spectroscopy methods, *J. Electron Spectrosc. Relat. Phenom.*, 195, 145–154.

[40] Kumar, V., Kumar, A., Lee, D.J., and Park, S.S., 2021, Estimation of number of graphene layers using different methods: A focused review, *Materials*, 14 (16), 4590.

[41] Paredes, J.I., Villar-Rodil, S., Martínez-Alonso, A., and Tascón, J.M.D., 2008, Graphene oxide dispersions in organic solvents, *Langmuir*, 24 (19), 10560–10564.

[42] Ding, H., Zhang, S., Chen, J.T., Hu, X.P., Du, Z.F., Qiu, Y.X., and Zhao, D.L., 2015, Reduction of graphene oxide at room temperature with vitamin C for RGO-TiO$_2$ photoanodes in dye-sensitized solar cell, *Thin Solid Films*, 584, 29–36.

[43] Tammer, M., 2004, G. Sokrates: Infrared and Raman characteristic group frequencies: Tables and charts, *Colloid Polym. Sci.*, 283 (2), 235.

[44] Lotfi, M., Yari, H., Sari, M.G., and Azizi, A., 2022, Fabrication of a highly hard yet tough epoxy nanocomposite coating by incorporating graphene oxide nanosheets dually modified with amino silane coupling agent and hyperbranched polyester-amide, *Prog. Org. Coat.*, 162, 106570.

[45] Sahoo, P., Shubhadarshinee, L., Jali, B.R., Mohapatra, P., and Barick, A.K., 2021, Synthesis and characterization of graphene oxide and graphene from coal, *Mater. Today: Proc.*, 56, 2421–2427.

[46] Fadillah, G., Saleh, T.A., Wahyuningsih, S., Ninda Karlina Putri, E., and Febrianastuti, S., 2019, Electrochemical removal of methylene blue using alginate-modified graphene adsorbents, *Chem. Eng. J.*, 378, 122140.

[47] Cao, H., Wu, X., Yin, G., and Warner, J.H., 2012, Synthesis of adenine-modified reduced graphene oxide nanosheets, *Inorg. Chem.*, 51 (5), 2954–2960.

[48] Liu, F., Cao, Y., Yi, M., Xie, L., Huang, W., Tang, N., Zhong, W., and Du, Y., 2013, Thermostability, photoluminescence, and electrical properties of reduced graphene oxide-carbon nanotube hybrid materials, *Crystals*, 3 (1), 28–37.

[49] Geng, J., Liu, L., Yang, S.B., Youn, S.C., Kim, D.W., Lee, J.S., Choi, J.K., and Jung, H.T., 2010, A simple approach for preparing transparent conductive graphene films using the controlled chemical reduction of exfoliated graphene oxide in an aqueous suspension, *J. Phys. Chem. C*, 114 (34), 14433–14440.

[50] Eda, G., and Chhowalla, M., 2010, Chemically derived graphene oxide: Towards large-area thin-film electronics and optoelectronics, *Adv. Mater.*, 22 (22), 2392–2415.

[51] Fadillah, G., Wicaksono, W.P., Fatimah, I., and Saleh, T.A., 2020, A sensitive electrochemical sensor based on functionalized graphene oxide/SnO_2 for the determination of eugenol, *Microchem. J.*, 159, 105353.

[52] You, S., Luzan, S.M., Szabó, T., and Talyzin, A.V., 2013, Effect of synthesis method on solvation and exfoliation of graphite oxide, *Carbon*, 52, 171–180.

[53] Jung, I., Field, D.A., Clark, N.J., Zhu, Y., Yang, D., Piner, R.D., Stankovich, S., Dikin, D.A., Geisler, H., Ventrice, C.A., and Ruoff, R.S., 2009, Reduction kinetics of graphene oxide determined by electrical transport measurements and temperature programmed desorption, *J. Phys. Chem. C*, 113 (43), 18480–18486.

[54] Tambe, P., 2021, Synthesis and characterization of acid treated reduced graphene oxide, *Mater. Today: Proc.*, 49, 1294–1297.

[55] Chasanah, U., Trisunaryanti, W., Triyono, T., Oktaviano, H.S., and Fatmawati, D.A., 2021, The performance of green synthesis of graphene oxide prepared by modified Hummers method with oxidation time variation, *Rasayan J. Chem.*, 14 (3), 2017–2023.